

A Miniaturization Technique of a Compact Omnidirectional Antenna

Sarah SUFYAR, Christophe DELAVEAUD

CEA-LETI MINATEC F-38054 Grenoble, France

sarah.sufyar@cea.fr, christophe.delaveaud@cea.fr

Abstract. This paper discusses a miniaturization technique of a compact omnidirectional antenna. A slot loading technique is applied to a well-known low-profile antenna structure whose radiation characteristics are similar to equivalent monopole ones. An equivalent circuit which models the antenna input impedance including the slot effect is also developed in order to illustrate the antenna working principle. The typical dimensions (width \times height) of the obtained antenna are $\lambda_0/11 \times \lambda_0/75$ (λ_0 is the free space operating wavelength) which makes it a miniature antenna that can be integrated inside small wireless sensor nodes using narrow band communication systems. Its performances are in accordance with classical fundamental limits, the operating bandwidth and efficiency are significantly reduced with the antenna size reduction.

Keywords

Omnidirectional radiation, miniaturization, slot loading, fundamental limits.

1. Introduction

Antenna miniaturization is an old and well documented topic regularly completed by recent advances in the antenna literature [1], [2]. Telecommunication system developments have been a major motivator of small antenna research during the last decade, most particularly for mobile terminals. The study of new Wireless Sensor Networks is generating a need for new kinds of aeri- als whose radiating properties are critical from the network communicating strategy. In particular, for compact sensors devices operating at low UHF frequencies, a strong constraint is placed on the antenna miniaturization and integration inside node structure.

This paper deals with a miniaturization technique applied to a compact antenna structure. The initial antenna structure, which is classically considered either as a top loaded folded monopole or as a shorted microstrip antenna [3], constitutes a compact low-profile antenna with typical larger length of $\lambda_0/6$ (λ_0 being the free space operating wavelength) and a height of $\lambda_0/20$, depending on the wished operating bandwidth. Numerous developments

have been carried out to improve and extend the antenna performances. Wide band [4], [5] and more recently Ultra Wide Band properties [6] have been demonstrated. Other important developments such as multiband behavior [7] or multi-function capabilities [8] have been obtained using this antenna concept. Since the antenna structure is electrically small, few works dealing with its size reduction are available in the literature. However, as a classical down- sizing technique, miniaturization attempts have been per- formed using high permittivity material as antenna sub- strate [9]. Another solution to reduce the size of such an antenna is proposed in this paper. Among the numerous miniaturization techniques available in the literature, slot loading technique is a classical solution used to size reduc- tion, bandwidth enlargement and multi-band operation mode of microstrip patch antennas [10]. This technique is applied to the particular antenna structure whose operating mode significantly differs from classical patch antennas. It can be equally highlighted that the use of slot has already been studied with this antenna structure but with the objec- tive of dual band behavior [11].

The studied antenna geometry is depicted in Sec- tion 2. The next section presents the slot loading effect on antenna impedance and radiation properties using experi- mental results and 3D electromagnetic simulation tools. In Section 4, the antenna behavior is firstly analyzed by proposing an equivalent circuit which simulates the antenna impedance at low frequencies. Then the antenna miniaturization is discussed using typical criteria of miniature antennas such as quality factor, frequency bandwidth, efficiency and antenna volume. The antenna properties functions of size reduction are compared to the classical well-known fundamental limits of electrically small antennas.

2. Antenna Geometry

The basic studied antenna structure is commonly known as a top loaded folded monopole or a shorted microstrip antenna [3]. The latter is very interesting for application in numerous wireless devices due to its compact size, low profile and omnidirectional radiation properties. Hence, it constitutes an attractive structure whose properties can evolve with the communication

system requirements. The studied antenna geometry is depicted in Fig. 1. It presents the simplest configuration of the Monopolar Wire Patch antenna. The metallic top hat is short circuited by a cylindrical conductor which introduces a low frequency parallel resonance where the new operating mode is obtained. The top hat is etched on a 0.8 mm thick FR4 substrate ($\epsilon_r = 4.4$, $\tan\delta = 0.018$) acting as mechanical support. The antenna has typical larger dimension of $\lambda_0/6.5$ (λ_0 being the free space operating wavelength). The dielectric substrate supporting the antenna hat is hanging up at a short distance ($\lambda_0/45.5$) from the ground plane by four spacers. The ground plane of significant dimensions compared to the operating frequency is centered below the antenna to efficiently act as classical electrical mirror (electrical image theory for monopole). Moreover, its size is chosen to limit reduced ground plane effects during experiments.

By cutting a slot in the metallic top hat, the low frequency resonating mode is modified and is most particularly shifted towards low frequencies. Indeed, by using a particular configuration of the slot (Fig. 1), a significant reduction of the resonant frequency associated to the operating mode can be obtained. The frequency shift is strongly dependent on the slot length. This behavior is illustrated and analyzed in the following sections.

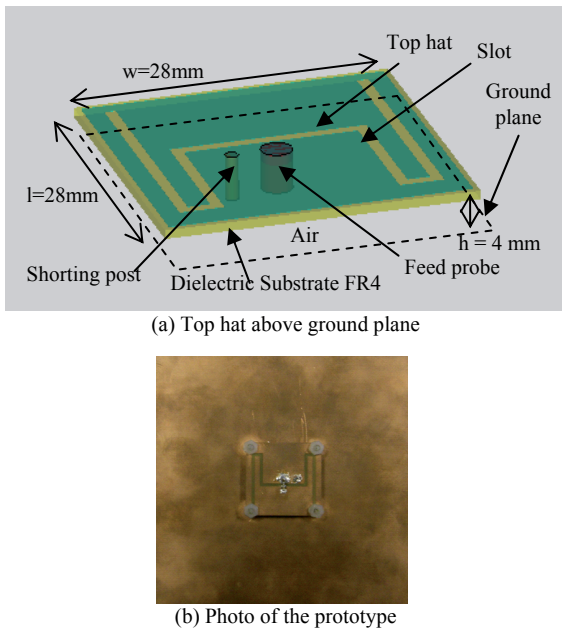


Fig. 1. Description of the antenna structure.

3. Slot Loading Effect

To study the slot effect, simulations and experiments were simultaneously carried out. In a first step, the impedance matching to 50 Ohms was not considered and only the behavior of the antenna input impedance in the vicinity of low frequency resonance mode (associated to the shorting wire) was studied. Among the numerous configurations of

simulated structures, three different prototypes were fabricated for experimental validation of simulated results: one without a slot, one with a slot length of (L_s) 50.5 mm and another one of 89.5 mm length. Measurement results are compared to simulated ones in order to validate the antenna behavior and the associated performances.

3.1 Input Impedance

The evolution of the input impedance (real and imaginary parts) is presented for different slot lengths (L_s). Simulation and measurement results are compared in Fig. 2. The low frequency resonance for different slot lengths is very similar in simulation and measurement. The introduction of the slot shifts the parallel resonance towards low frequencies. It can be equally assumed that the low resonance frequency is decreasing as the slot length is increasing.

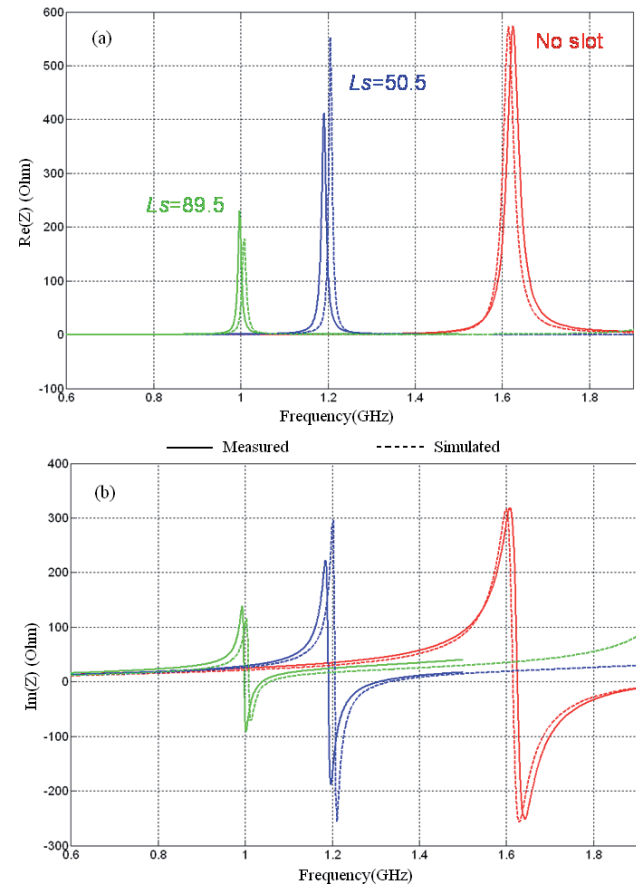


Fig. 2. Evolution of the low frequency resonance versus slot length (L_s in mm) in simulation and measurement.

3.2 Intrinsic Gain Diagrams

The radiation properties of the antenna including the slot in the top hat are studied using 3D electromagnetic simulation tool [12] and by measuring the radiation pattern plus the intrinsic gain of prototypes (impedance mismatching is not taken into account). Fig. 3 compares the simulated and measured gain diagrams for different slot

configurations in two orthogonal cut planes (see Fig. 3 for cut plane definition). The radiation properties are plotted at the parallel resonance frequency f_r associated to each slot length. For the basic antenna structure, the curves are quite identical and the gain at horizon (P1 cut plane, Fig. 3 (a)) is around 0 dBi.

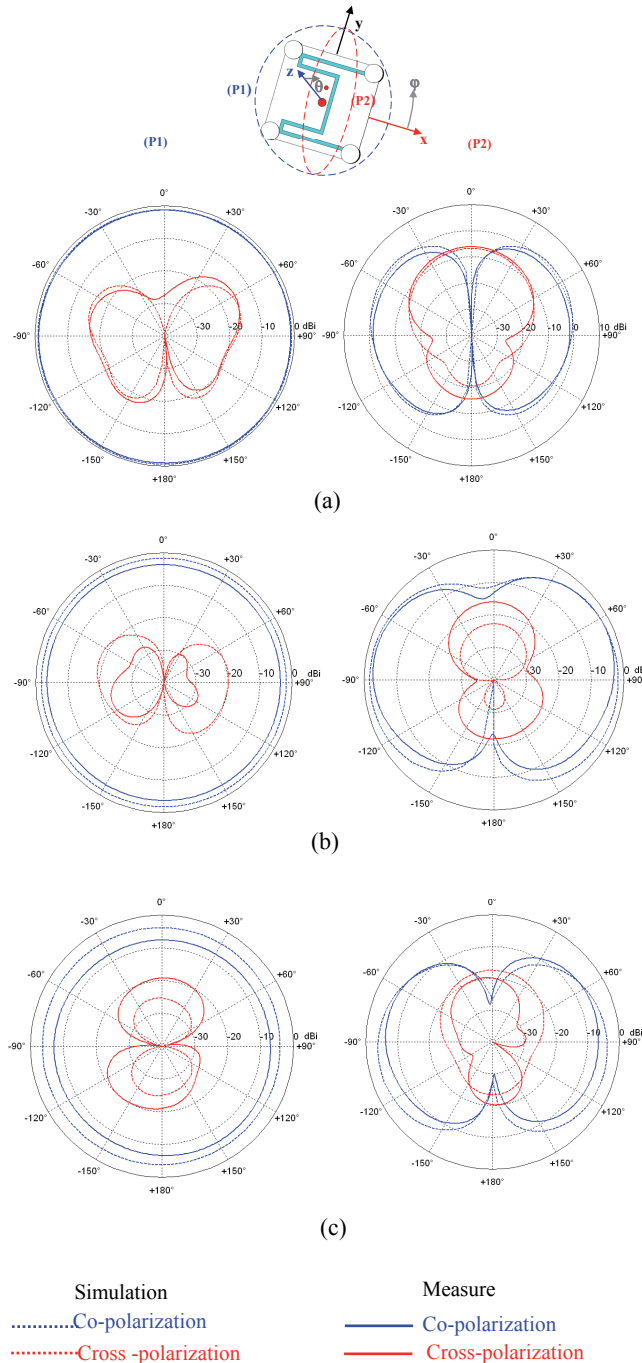


Fig. 3. Gain diagrams in simulation and measurement for different slot configurations: (a) No slot, (b) $L_s = 50.5$ mm, (c) $L_s = 89.5$ mm.

Some more obvious differences are observable between measurement and simulation results when slot is cut in the top hat. These discrepancies can be attributed to the difficulties to measure with accuracy the radiation properties of

the antenna when the frequency is lowered. As the frequency decreases, the electric size of the ground plane is reduced and the measurement cable could introduce some uncertainties on the measured radiation properties. The maximum measured intrinsic gain is around -4 dBi for $L_s = 50.5$ mm and -8 dBi for $L_s = 89.5$ mm. The classical Monopolar Wire Patch antenna has a typical diagram shape identical to the equivalent monopole antenna located over the same ground plane (i.e. dipolar shape in our case of limited ground plane). The omnidirectional properties of the antenna radiation with vertical main polarization of the field are quite preserved in the presence of the slot in the top hat.

The results obtained by measurements validate the ones obtained by simulations. The maximum gain is roughly of the same order and decreases as the frequency reduces.

4. Antenna Miniaturization

4.1 Miniaturization Factor

From the canonical compact antenna structure, the influence of the slot is thoroughly analyzed using 3D electromagnetism simulation tools [12]. Fig. 4 shows how the low frequency parallel resonance is modified by the slot length.

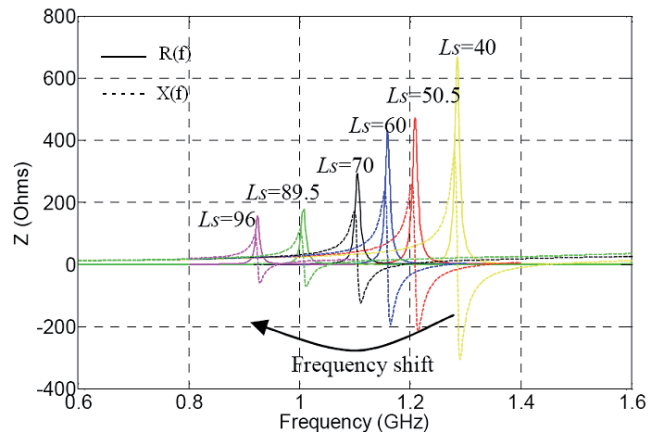


Fig. 4. Change of the low frequency antenna resonance versus slot length (L_s in mm) – simulated results.

The evolution of the resonance frequency f_r versus the slot length is displayed in Fig. 5. For comparison, the fundamental half wavelength mode of the slot, printed on the dielectric substrate, is equally plotted in Fig. 5. Being situated at higher frequencies, this resonating mode does not interfere with the low frequency resonance of the antenna. It confirms the non alteration of the slot on the radiation properties of the antenna.

Consequently, the frequency shift introduced by the slot loading can be interpreted as an increase of the equivalent capacitance of the antenna hat. This phenomenon is illustrated in the following subsection. In matching

the input impedance to 50 ohms in the vicinity of the shifted resonance, the antenna structure including the slot is hence miniaturized. The initial antenna structure has typical larger dimension of $\lambda_0/6.5$ and a height of $\lambda_0/45.5$. For $L_s = 90$ mm, the larger dimension is $\lambda_0/11$ and the height is $\lambda_0/75$. A frequency downshift of up to 40% of the low resonance frequency is noticed thanks to the presence of the slot.

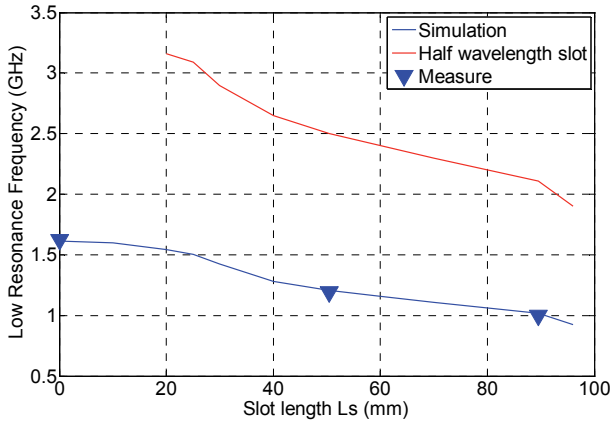


Fig. 5. Low resonance frequency (f_r) versus the slot length.

4.2 Slot Effect Modeling

To confirm the physical interpretation of the studied miniaturization technique, some developments of an equivalent circuit of the shorted microstrip antenna have been carried out. This equivalent circuit, already developed in [13], simulates the antenna impedance below the fundamental mode of the patch antenna. This electrical model is valid for antenna having low permittivity substrate above infinite ground plane. A simple model of slot has been introduced in the equivalent circuit to study the slot loading effect.

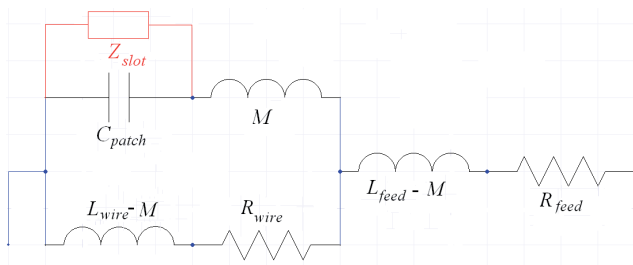


Fig. 6. Low frequency circuit model of antenna impedance with slot effect.

The antenna impedance below the fundamental mode of the antenna is determined by different constitutive elements of the antenna, as illustrated in Fig. 6.

For classical probe fed patch antenna, the impedance is given by the capacitance of the antenna C_{patch} (constituted by the upper plate above the ground plane) in series with the feed probe inductance L_{feed} .

The capacitance value due to this kind of rectangular microstrip capacitor is defined as [14]:

$$C_{patch} = \frac{\epsilon_0 \epsilon_r W L}{h} + 2.Ce_1 + 2.Ce_2 \quad (1)$$

where Ce_1 and Ce_2 are respectively the edge capacitance along width W and length L of the resonator (i.e. top hat); h is the substrate thickness and ϵ_r being the relative permittivity of the substrate.

$$Ce_1 = \frac{1}{2} \left[\frac{1}{v_{\phi 1} Z(W, h, \epsilon_r)} - \frac{\epsilon_0 \epsilon_r W}{h} \right] L \quad (2)$$

$$Ce_2 = \frac{1}{2} \left[\frac{1}{v_{\phi 2} Z(L, h, \epsilon_r)} - \frac{\epsilon_0 \epsilon_r L}{h} \right] W \quad (3)$$

$v_{\phi 1}$ ($v_{\phi 2}$) represents the phase velocity of the quasi TEM mode propagating along the microstrip line of width W (L)

$$v_{\phi 1} = c \frac{Z(W, h, \epsilon_r)}{Z(W, h, 1)} \quad (4)$$

$$v_{\phi 2} = c \frac{Z(L, h, \epsilon_r)}{Z(L, h, 1)} \quad (5)$$

$Z(x, h, \epsilon_r)$ is the characteristic impedance of the microstrip line of width x [15]:

$$Z(x, h, \epsilon_r) = \frac{120 \pi}{\sqrt{\epsilon_e}} \left[\frac{x}{h} + 1,393 + 0,667 \ln \left(\frac{x}{h} + 1,441 \right) \right]^{-1}, \quad (6)$$

$$\epsilon_e = \frac{\epsilon_r + 1}{2} + \frac{\epsilon_r - 1}{2} \left(1 + 12 \frac{h}{w} \right)^{-\frac{1}{2}} \quad \text{if } \frac{h}{w} < 1. \quad (7)$$

For a square form patch, the inductance of the coaxial probe is expressed as follow [16]:

$$L_{feed} = \frac{\mu_0 h}{2 \pi} \ln \left(\frac{2c}{\pi \gamma r \sqrt{\epsilon_r} f} \right). \quad (8)$$

where r is the radius of the probe, c the light velocity, γ is Euler constant (1.781), h is the probe length.

Then, the ground wire, that connects the patch to the ground plane, acts as a short circuit to the antenna capacitance. This element is set in parallel to the antenna capacitance and introduces the low frequency resonance [13]. The ground wire inductance is derived using the coaxial probe inductance formula (8), r is the ground wire radius.

Besides, a mutual inductance M is introduced to take into account the coupling between the inductances. The expression is set in [13] as follow:

$$M = \frac{\mu_0 h}{2 \pi} \ln \left(\frac{c}{\pi \gamma d \sqrt{\epsilon_r} f} \right). \quad (9)$$

d is the distance between the wires axis.

Losses are introduced by the radiation resistances R_{feed} and R_{wire} of wires. The radiation resistances are defined by the expression given in [18]:

$$R = 240 \pi^2 \left(\frac{hf}{c} \right)^2 I(h, f, \epsilon_r), \quad (10)$$

$$I(h, f, \epsilon_r) = \int_{-\pi/2}^{\pi/2} \frac{\cos^2 \theta \sin^3 \theta}{\epsilon_r^2 \cos^2(\Psi_0 h) \cos^2 \theta + (\epsilon_r - \sin^2 \theta) \sin^2(\Psi_0 h)} d\theta, \quad (11)$$

$$\Psi_0 = 2\pi \frac{f}{c} \sqrt{\epsilon_r - \sin^2 \theta}. \quad (12)$$

The described equivalent electrical circuit with the associated analytical formulation of its components constitutes the reference circuit to introduce the slot effect. The antenna geometry is simplified for this analysis due to electrical circuit limitations (large ground plane and air as dielectric substrate). By cutting a slot in the antenna patch, the antenna capacitance is mainly modified. This effect can be modeled by introducing the slot complex impedance in parallel to the antenna capacitance (Fig. 6). To highlight the slot effect, a simple slot impedance model is introduced in the equivalent circuit. Hypothesis on the calculation of this model limit the geometry of the slot, as shown in the Fig. 7. Further modeling works are required to improve the slot impedance model (position of the slot, proximity of the ground plane, bent slot shape). However, the basic approach provides interesting results, most especially concerning the evolution of resonant frequency versus slot length.

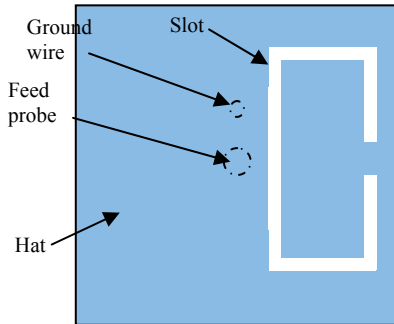


Fig. 7. Structure of the slot in the antenna hat for the electrical circuit modeling.

The impedance of a slot has been calculated using [17]. For a simple straight slot (Fig. 8.) in a ground plane, the Babinet principle defining the equivalent dipole antenna has been used to obtain the electrical and magnetic fields of the slot. The calculation of the electromagnetic fields allows the calculation of the input admittance of the slot.

The slot admittance is given by :

$$Y_s = G_s + jB_s \quad (13)$$

where G_s is the conductance of the slot and B_s is the susceptance. First, the radiated power is evaluated along the $y > 0$, in the YZ plane at (r_c, θ) point, which is given in [17] (r_c and θ are the cylindrical coordinates):

$$P(r_c, \theta) = \frac{1}{2} \frac{1}{120\pi} E_\phi^2. \quad (14)$$

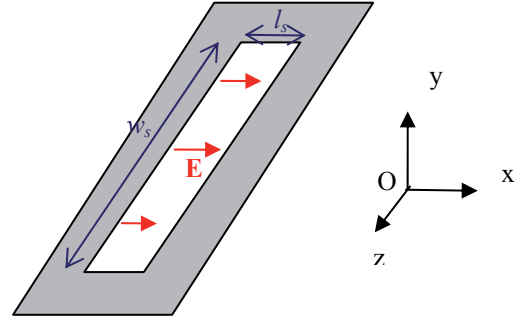


Fig. 8. Slot excited by an electric field.

By developing this expression, we obtain:

$$P(r_c, \theta) = \frac{1}{2} \frac{1}{120\pi} \frac{V_0^2}{\pi} \int_0^{2\pi} \frac{\sin^2 \left(\frac{\pi \cdot w_s}{\lambda_0} \cos \theta \right)}{\cos^2 \theta} \sin^2 \theta \cdot \sin \theta \cdot d\theta. \quad (15)$$

Knowing that the radiating power is function of G_s :

$$P(r_c, \theta) = \frac{1}{2} V_0^2 G_s. \quad (16)$$

V_0 is the potential between slot sides.

By combining (15) and (16), we can deduce the expression of G_s . Assuming that $\frac{w_s}{\lambda_0} \ll 1$, the simplified formula is:

$$G_s = \frac{1}{90} \left(\frac{w_s}{\lambda_0} \right)^2. \quad (17)$$

Finally, the susceptance is determined knowing the input impedance of a short-circuited microstrip line equivalent to a capacitive stub with a length of Δl [17]:

$$B_s = \frac{2\pi}{\lambda_0} \Delta l \sqrt{\epsilon_e} \frac{1}{Z_c}. \quad (18)$$

with:

$$Z_c = \frac{120\pi}{\sqrt{\epsilon_e}} \frac{l_s}{w_s} \quad \text{if} \quad \frac{l_s}{w_s} \ll 1 \quad (19)$$

and the length is given:

$$\Delta l = 0.412 l_s \frac{\epsilon_e + 0.3}{\epsilon_e - 0.258} \left(\frac{\frac{w_s}{l_s} + 0.264}{\frac{w_s}{l_s} + 0.8} \right). \quad (20)$$

The effective permittivity is given by (7).

Hence the slot impedance (admittance) can be calculated and introduced in the antenna equivalent circuit. Fig. 9 compares the evolution of the low antenna resonance frequency obtained with 3D electromagnetic software [12] and the equivalent circuit. Similar evolutions of the resonant frequency are observed with both tools. The higher the length is, the lower the resonance frequency is. The simulation results are in a good agreement with the modeling, in spite of the crude slot model. These results con-

firm the physical interpretation of the slot loading technique of this kind of compact antenna.

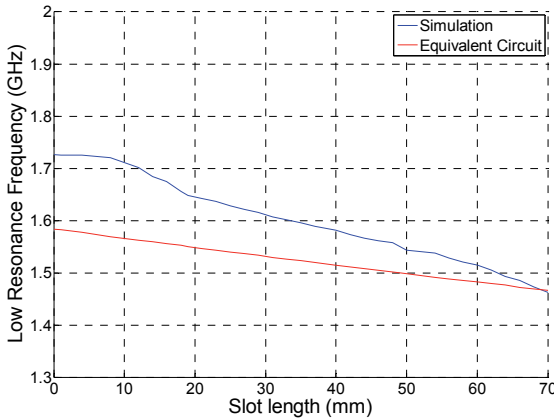


Fig. 9. Evolution of the low resonance frequency (f_r) versus slot length.

4.3 Quality Factor and Bandwidth

Different expressions of the quality factor of electrically small antennas can be found in the literature. The antenna behavior is studied using the quality factor Q defined in [19]. It is derived from the antenna impedance:

$$Q = \frac{\omega_0}{2R_0(\omega_0)} |Z'_0(\omega_0)|. \quad (21)$$

where R_0 is the real part of the complex impedance, Z'_0 is the derivative of the complex impedance and ω_0 is the radian frequency. This expression was applied to the antenna impedance having different slot lengths. In Tab. 1, we present the values obtained at the low frequency antenna resonance f_r . The associated maximum frequency bandwidth (FBW) defined for a VSWR (s) of 2 is equally reported in last columns. This parameter is derived using the following formula [19].

$$FBW|_{s=2} = \frac{2\sqrt{\beta}}{Q} \text{ where } \sqrt{\beta} = \frac{s-1}{2\sqrt{s}} \leq 1. \quad (22)$$

A correct agreement is obtained between simulation and measurement results.

The published reference works dealing with fundamental limits of electrically small antenna propose a well-known law which links together antenna dimensions, minimum Q factor and efficiency [20], [21].

Slot length (mm)	f_r (GHz)		Q		FBW (%)	
	Sim.	Meas.	Sim.	Meas.	Sim.	Meas.
0	1.614	1.625	55	46.7	2.16	1.83
50.5	1.209	1.191	107.4	95.9	1.11	1.2
89.5	1.016	0.997	112.2	107.7	1.06	1.1
96	0.925	-	112.6	-	1.05	-

Tab. 1. Evaluation of Q and FBW for different values of the low frequency antenna resonance f_r .

The minimum quality factor for a single lowest TE (TM) mode of a compact lossless radiating structure included inside a sphere of radius a is given by :

$$Q_{\min} = \frac{1}{k^3 a^3} + \frac{1}{ka}. \quad (23)$$

k is the wave vector.

The dependence of Q [19] versus antenna dimension is illustrated in Fig. 10. The considered sphere radius to define the antenna dimension is the half diagonal of the antenna hat. This choice can be discussed due to the equivalent monopole antenna behavior. Indeed, we make the hypothesis that the ground plane is large enough not to alter the antenna behavior when frequency is decreased. For comparison, the minimum Q [20] ($\eta=100\%$) is plotted in Fig. 10. As classically observed, the antenna Q is much higher than the theoretical limit. Q values increase as the antenna size decreases. Simulated and measured results show similar behaviors.

Assuming the bandwidth proportional to the inverse of Q factor, the bandwidth is consequently narrowing with the antenna miniaturization. This behavior is in accordance with the fundamental limits of electrically small antennas.

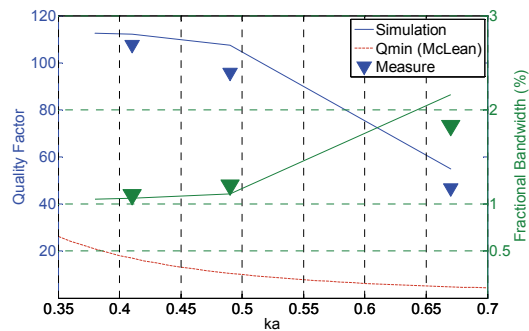


Fig.10. Quality factor and fractional frequency bandwidth versus antenna dimension (ka).

4.4 Efficiency

The efficiency is a critical parameter of electrically small antennas. The antenna radiation efficiency was calculated with a 3D electromagnetism simulation tool [12] and was measured using the Wheeler Cap method [22].

The obtained results are compared in Tab. 2. A good agreement is obtained between simulation and measurement results.

Slot length (mm)	Efficiency (%)	
	Simulation	Measurement
0	78	77
40	43	-
50.5	35.6	36
60	30	-
89.5	29.2	27.8

Tab.2. Efficiency calculated by simulation and measured with the Wheeler Cap method.

Efficiency is plotted versus antenna size in Fig. 12. Efficiency is clearly reduced with the antenna size in both simulation and measurement. The antenna performances are hence in accordance with the fundamental limits.

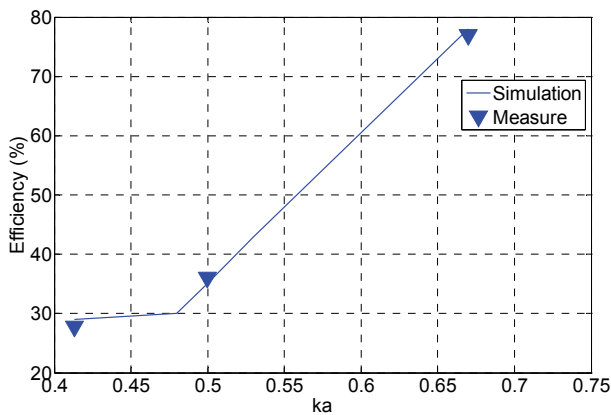


Fig. 12. Efficiency versus antenna dimension (ka).

4.5 Bandwidth, Efficiency and Antenna Volume

For very compact antennas having $a \ll \lambda_0/2\pi$, the fundamental limits can be reduced as follow:

$$\eta \cdot \frac{1}{Q} \approx (ka)^3 \tag{24}$$

η being the antenna radiation efficiency.

This formula indicates that Quality factor (bandwidth), efficiency and antenna volume are linked together. More precisely, the product of antenna bandwidth with efficiency is proportional to the antenna volume. To estimate the validity of this relation, Tab. 3 proposes the calculation of $\eta/Q(ka)^3$ for different slot lengths. The ratio does not seem to be constant. Actually, the hypothesis on the antenna size is not fully verified. However, as the antenna size is reducing, the calculated values tend to be more stable. Additional simulated and measured results will be helpful to validate any conclusion.

Slot length (mm)	ka	$\frac{\eta}{Q(ka)^3}$	
		Simulation	Measurement
0	0.67	0.047	0.054
50.5	0.5	0.027	0.032
89.5	0.41	0.034	0.036

Tab.3. Link between bandwidth, efficiency and the volume occupied by the antenna.

5. Conclusion

A slot loading technique has been successfully applied to reduce the size of a compact omnidirectional antenna. The slot effect has been carefully analyzed using

3D electromagnetic simulation tool and modeled using a simple equivalent circuit. The presented miniaturization technique leads to a low cost miniature antenna with performances in accordance with classical fundamental antenna limits. Operating bandwidth and antenna efficiency significantly reduce with the antenna dimensions. Such antenna structure has been developed to be integrated inside small wireless sensor node demonstrator. This device uses narrow band communication systems (low data rate, low power system) for prevention and detection of forest fire and landslide.

Acknowledgements

This study was done in the framework of the WinSoc project (FP6-2005-IST-5).

References

- [1] FUJIMOTO, K., HENDERSON, A., HIRASAWA, K., JAMES, J.R. *Small Antennas*. New York: John Wiley and Sons, Research Studies Press, 1987.
- [2] HANSEN, R.C. *Electrically Small Superdirective and Superconducting Antennas*. Hoboken, New Jersey: Wiley, 2006.
- [3] DELAVEAUD, C., LEVEQUE, P., JECKO, B. Small-sized low-profile antenna to replace monopole antennas. *Electronics Letters*, 16 Apr 1998, vol. 34, no. 8, p. 716-717.
- [4] LAU, KL., LI, P., LUK, KM. A monopolar patch antenna with very wide impedance bandwidth. *IEEE Transactions on Antennas and Propagation*, 2005, vol. 53, no. 3, pp 1004- 1010.
- [5] ROW, J. S., YEH, S. H., WONG, K. L. A wide-band monopolar plate-patch antenna. *IEEE Transactions on Antennas and Propagation*, 2002, vol. 50, no. 9, pp. 1328-1330.
- [6] BOURTOUTIAN, R., DELAVEAUD, C., TOUTAIN, S. Low profile UWB monopole antenna having a sharp band notch function. In *European Conference on Antennas and Propagation (EuCAP2006)*. Nice (France), 2006.
- [7] ZAID, L., STARAJ, R. Miniature circular GSM wire-patch antenna on small ground plane. *Electronics Letters*, 14 Feb 2002, vol. 38, no. 4, pp 153-154.
- [8] JECKO, B., DECROZE, C. The ‘Monopolar Wire Patch Antenna’ concept. In *Second European Conference on Antennas and Propagation, EuCAP 2007*, 11-16 Nov. 2007, pp 1-5.
- [9] PASQUET, F., JECKO, B. New developments of the wire-patch antenna for ceramic technology and multifunction applications. In *I.E.E.E. Antennas and Propagation Society International Symposium*, 8-13 July 2001, vol. 4, pp 62 – 65.
- [10] WONG, K.L. *Compact and Broadband Microstrip Antennas*. New York: J. Wiley & Sons, Inc., Wiley Series in Microwave and Optical Engineering.
- [11] JECKO, F., HAMMOUDI, M. *Multi Frequencies Wire Patch Antenna (Antenne fil-plaque Multifréquence)*. French patent, n° 01 07940, December 2002.
- [12] MICROWAVE STUDIO, *Computer Simulation Technology*, <http://www.cst.de>.

- [13] DELAVEAUD, C. New kind of microstrip antenna: the monopolar wire-patch antenna (Etude d'une nouvelle classe d'antenne imprimée a rayonnement monopolaire). *PhD dissertation*, University of Limoges, Oct. 1996.
- [14] WOLFF, I., KNOPPIK, N. Rectangular and circular microstrip disk capacitors and resonators. *I.E.E.E. Trans. on Microwave Theory and Techniques*, October 1974, vol. 22, no. 10.
- [15] WHEELER, H. A. Transmission-line properties of parallel strips separated by a dielectric sheet. *I.E.E.E. Trans. on Microwave Theory and Techniques*, March 1965, vol. 13, pp. 172-185.
- [16] LIER, E. Improved formulas for input impedance of coax-fed microstrip patch antennas. *I.E.E. Proc.*, August 1982, pp. 161-164.
- [17] COMBES, P.F. *Micro-ondes, circuits passifs, propagation, antennes*. DUNOD, Tome 2, 1997.
- [18] CHI, C.L., ALEXOPOULOS, N.G. Radiation by a probe through a substrate. *IEEE Trans. Antennas and Propagation*, September 1986, vol. 34, no. 9, pp. 1080-1091.
- [19] YAGHJIAN, A. D., BEST, R. Impedance, bandwidth, and Q of antennas. *IEEE Trans. Antennas and Propagation*, April 2005, vol. 53, no. 4, pp.1298-1324.
- [20] MCLEAN, J. S. A re-examination of the fundamental limits on the radiation Q of electrically small antennas. *IEEE Trans. Antennas and Propagation*, May 1996, vol. 44, pp. 672-675.
- [21] HARRINGTON, R. F. Effect of antenna size on gain, bandwidth and efficiency. *J. Res. Natl. Bur. Stand.*, Jan./Feb. 1960, vol. 64-D, pp. 1-12.
- [22] MCKINZIE, W. E. A modified Wheeler cap method for measuring antenna efficiency. In *IEEE Antennas Propagat. Soc. Int. Symp. Dig.*, Jul. 1997, vol. 1, pp. 542-545.

About Authors

Sarah SUFYAR was born in Bordeaux, France in 1985 and received an engineering and Master's degree in Electronics from ENSEIRB, Electronics Engineering School in Bordeaux, France. She is a first year PhD student at CEA-LETI MINATEC, France and works on reconfigurable miniature antennas since 2008.

Christophe DELAVEAUD obtained his PhD in high frequency electronics from the University of Limoges, France, in 1996. From 1991 to 1997, he was a Teaching Assistant at the University Institute of Technology in Limoges, France. In 1998, he moved to the European R & D centre of Radiall / Larsen Antenna Technology in Voreppe, France. He was responsible for developing new antenna concepts, with the emphasis on miniature antennas, wide-band and multi-band antennas for customer applications in wireless communications. Since 2000, he has been a visiting lecturer at the University of Savoie, Chambéry, France. In 2002, he joined the Atomic Energy Commission (CEA), Laboratory of Electronics and Information Technology (LETI), Grenoble, France, as Senior Researcher. His current research interests include the analysis and development of radiating structures, with an emphasis on miniature integrated antennas, multi-antenna systems, ultra-wide band antennas and smart antennas for wireless communications systems.